BIOCHEMISTRY
including biophysical chemistry & molecular biology

Article

pubs.acs.org/biochemistry

Molecular Basis for the Mechanism of Constitutive CBP/p300 Coactivator Recruitment by CRTC1-MAML2 and Its Implications in cAMP Signaling

Michael David Clark,[†] Ganesan Senthil Kumar,[†] Ryan Marcum,[†] Qianyi Luo,[†] Yongbo Zhang,[‡] and Ishwar Radhakrishnan*[,†]

[†]Department of Molecular Biosciences, Northwestern University, 2205 Tech Drive, Evanston, Illinois 60208-3500, United States
[‡]Department of Chemistry, Northwestern University, 2145 Sheridan Road, Evanston, Illinois 60208-3113, United States

Supporting Information

ABSTRACT: The cyclic AMP response element-binding protein (CREB) is a signal-dependent transcription factor that exerts its positive effects on gene transcription of a broad range of genes by recruiting coactivators, including CREB-binding protein (CBP), its paralog, p300, and the family of CRTC (CREB-regulated transcriptional coactivators) proteins. Whereas recruitment of CBP/p300 is dependent on CREB phosphorylation at Ser133, recruitment of CRTCs is not. Here we describe how both mechanisms could concurrently drive transcription of CREB targets in a subset of head and neck cancers featuring chromosomal translocations that fuse portions of *CRTC1* and *CRTC3* genes with that of the Mastermind-like transcriptional coactivator MAML2. We show that a peptide derived from transactivation domain 1 (TAD1) of MAML2 binds to the CBP KIX domain with micromolar affinity. An ∼20-residue segment within this peptide, conserved in MAML2 orthologs and paralogs, binds directly to a KIX surface previously shown to bind to MLL1. The 20-residue MAML2 segment shares sequence similarity with MLL1, especially at those positions in direct contact with KIX, and like MLL1, the segment is characterized by the presence of an ∼10-residue helix. Because CRTC1/3-MAML2 fusion proteins are constitutively nuclear, like CREB, our results suggest constitutive recruitment of CBP/p300 to CREB targets that could be further enhanced by signals that cause CREB Ser133 phosphorylation.

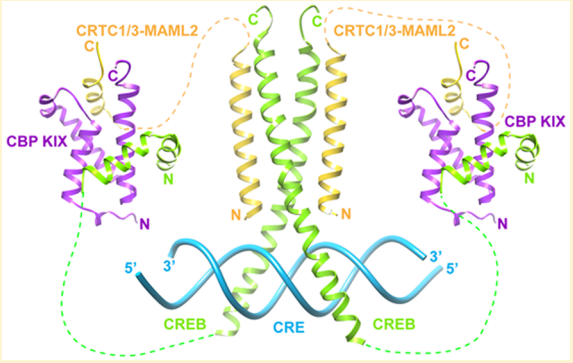

The cyclic AMP response element-binding protein (CREB) is the prototypical signal-dependent, sequence-specific DNA-binding transcriptional activator that regulates expression of a broad range of genes in response to increases in intracellular cAMP and Ca^{2+} levels caused by extracellular signals such as hormones and nutrients.[1,2] CREB exerts its positive effects on gene transcription by recruiting two families of transcriptional coactivators with intrinsic or associated lysine acetyltransferase (KAT) activities via distinct molecular mechanisms. Recruitment of the CBP/p300 family of coactivators relies on cAMP-activated, protein kinase A-mediated phosphorylation of a specific serine residue (Ser133) located in the kinase inducible transactivation domain (KID) of CREB.[3] Ser133 phosphorylation potentiates CBP/p300 recruitment via direct interactions of the KID with the CBP/p300 KIX domain.[4,5]

Recruitment of the CRTC family and their associated KAT, PCAF/KAT2B, occurs through a mechanism independent of CREB phosphorylation.[6−8] Members of the CRTC family comprising CRTC1, CRTC2, and CRTC3 are retained in an inactive, hyperphosphorylated form in complex with 14-3-3 proteins in the cytoplasm under basal conditions.[9] Elevations in the intracellular levels of cAMP and Ca^{2+} trigger the dephosphorylation and release of the CRTC proteins from 14-3-3 complexes. Following nuclear entry, the CRTC proteins associate via a conserved N-terminal helical segment with the DNA-bound basic leucine zipper (bZip) domain of CREB.[10]

Besides their well-established roles in promoting long-term memory and glucose homeostasis,[11−13] CRTC1 and CRTC3 have been implicated in a subset of mucoepidermoid carcinomas (head and neck cancers).[14,15] These cancers are characterized by recurrent chromosomal translocations that fuse the segment encoding the N-terminal CREB-binding domain (CBD) of CRTC1/3 with substantial portions of the coding regions of another coactivator called MAML2.

MAML2 is homologous to the Mastermind protein in *Drosophila* and along with MAML1 and MAML3 comprises the Mastermind-like family of transcriptional coactivators that play an important role in Notch signaling, regulating multiple developmental pathways.[16] Upon Notch activation, which results in the cleavage of the Notch receptor followed by translocation of

Received: March 28, 2015
Revised: August 13, 2015
Published: August 14, 2015

DOI: 10.1021/acs.biochem.5b00332
Biochemistry 2015, 54, 5439−5446

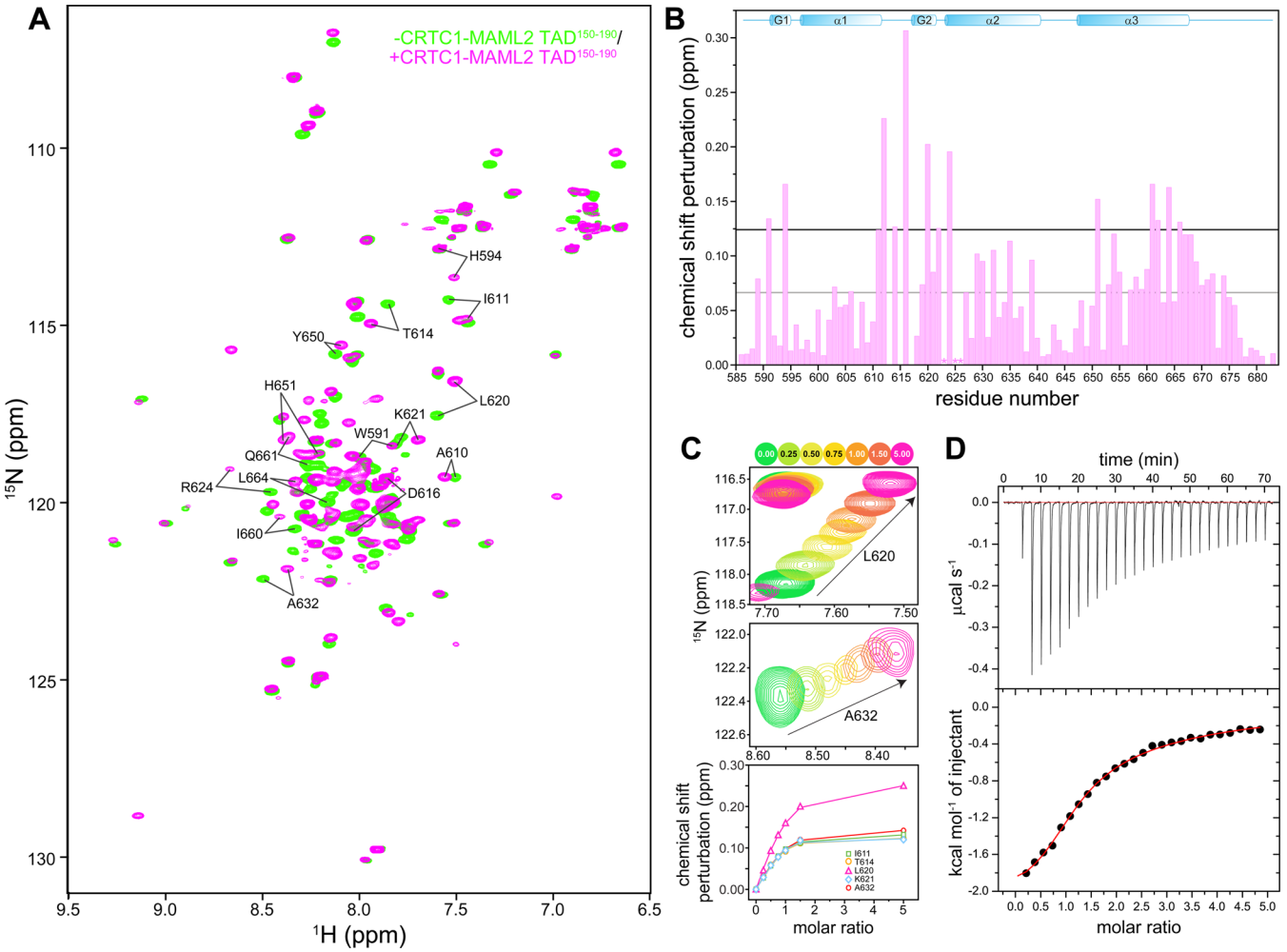

Figure 1. MAML2 transactivation domain that interacts with the KIX domain of CBP. (A) ^{1}H-^{15}N correlated spectra of mouse CBP KIX recorded in the absence (green) and presence (orange) of CRTC1-MAML2 TAD$^{150-190}$. (B) Backbone amide chemical shift perturbations (CSP) induced upon addition of 1 equiv of CRTC1-MAML2 TAD$^{150-190}$ polypeptide to a 0.75 mM NMR sample of KIX. The gray and black horizontal lines denote the average CSP and the average + one standard deviation of CSP induced in KIX, respectively. The asterisks denote residues with severely broadened resonances in the presence of the TAD. (C) Expanded plots of ^{1}H-^{15}N correlated spectra depicting changes to the positions of the L620 and A632 backbone resonances (top and middle panels) as a function of added TAD. Titrations were performed with 0.15 mM CBP KIX at 25 °C. Peaks are colored according to the number of added equivalents of TAD$^{150-190}$ (see the key at the top). The raw data (symbols; bottom panel) following quantification of the chemical shift changes are shown along with the fitted data (solid lines). (D) Representative binding isotherm from an ITC experiment showing association between the KIX and TAD polypeptides. KIX was in the cell, while the TAD$^{150-190}$ was in the syringe.

the intracellular domain to the nucleus, these coactivators bind via a conserved N-terminal basic domain to Notch as well as to the CSL family of DNA-binding factors, forming a ternary complex.[17] The MAML proteins harbor two acidic transactivation domains C-terminal to the basic domain, both of which are essential for the activation of Notch-regulated genes. Although the molecular target of the C-terminal TAD (TAD2) is presently unknown, TAD1 harbors a binding site for CBP/p300.

The CRTC1-MAML2 fusion protein (CRTC1-MAML2) lacks the 171 N-terminal residues, including the basic domain of MAML2, that are important for binding to Notch and CSL and all but the 42 N-terminal residues of CRTC1 corresponding to the CBD.[14] The protein thus lacks the nuclear export signals and regulatory domains of CRTC1 that are required for sequestration of CRTC in the cytoplasm. Like the MAML proteins, the resulting fusion protein is constitutively nuclear.[18] Previous studies have shown that CRTC1-MAML2 can function as a potent coactivator of CREB and that the transforming activity of the oncoprotein is due in large part to aberrant activation of CREB targets.[6,18] Additionally, one of the studies mapped a 175-residue segment within MAML2 TAD1 for efficient interactions with CBP/p300.[18] Deletion of this segment corresponding to residues 44−222 of CRTC1-MAML2 resulted in a level of induction of CREB target genes and transforming ability significantly reduced compared to those of the full-length protein, implying a central role for CBP/p300 in both processes.

EXPERIMENTAL PROCEDURES

Production of CBP KIX and CRTC1-MAML2 TAD Polypeptides. Mouse CBP KIX (residues 586−683) and CRTC1-MAML2 TAD1 (spanning residues 150−190 and 172−207; residue numbering follows that of the fusion protein and not that of native MAML2) constructs were produced by subcloning the respective segments in pMCSG7 and pMCSG23 vectors as His$_6$-tagged or His$_6$-MBP-tagged constructs. ^{15}N- and ^{13}C-labeled and unlabeled proteins were expressed in *Escherichia coli* and purified using Ni^{2+} affinity chromatography followed by removal of the tag by TEV protease and reversed-phase high-performance liquid

DOI: 10.1021/acs.biochem.5b00332
Biochemistry 2015, 54, 5439−5446

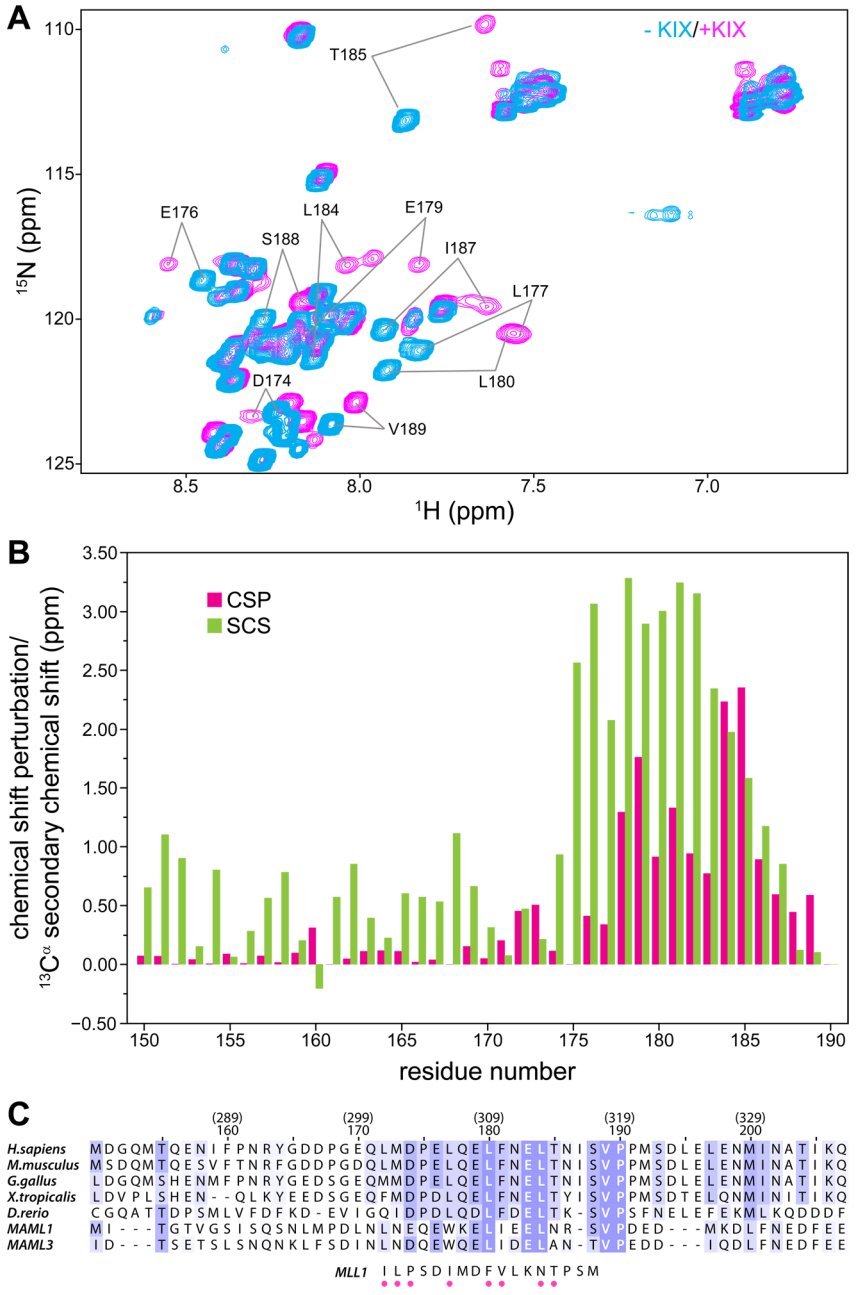

Figure 2. CRTC1-MAML2 TAD1 binds KIX via a short conserved, helical segment. (A) ^{1}H-^{15}N correlated spectra of ^{15}N- and ^{13}C-labeled CRCT1−MAML2 TAD$^{150-190}$ recorded in the absence (cyan) and presence (magenta) of 1 equiv of CBP KIX at 25 °C. (B) Backbone amide CSPs (green) for CRTC1-MAML2 TAD$^{150-190}$ induced by the addition of 1 equiv of KIX plotted as a function of residue number; the TAD concentration was 0.7 mM. CSPs were calculated as described in the legend of Figure 1B. Also graphed are $^{13}C^{\alpha}$ secondary chemical shifts (SCS; red) for TAD$^{150-190}$ when it is bound to KIX as a function of residue number. (C) CLUSTAL Ω-guided multiple-sequence alignment of MAML2 homologues from various species and comparison with the sequence of the MLL1 segment that engages KIX. The residue numbering in the context of human MAML2 is given in parentheses on top of the numbering in the context of the CRTC1-MAML2 fusion. Sequences were shaded on the basis of substitution scores from the BLOSUM62 scoring matrix in JalView.[31] MLL1 residues that make direct contacts with KIX in the NMR structure[25] are identified by dots below the sequence.

chromatography as described previously.[19] The identity and purity as well as the extent of isotope incorporation in the preparations were confirmed by mass spectrometry and sodium dodecyl sulfate−polyacrylamide gel electrophoresis (SDS−PAGE).

Nuclear Magnetic Resonance (NMR) Sample Preparation and Spectroscopy. NMR samples in the range of 0.7−0.75 mM were prepared in 50 mM sodium phosphate buffer (pH 6.0) containing 50 mM NaCl, 0.2% NaN_3, and 10% D_2O. Spectra were recorded at 35 °C on an Agilent DirectDrive 600 MHz spectrometer equipped with a pulsed-field gradient triple-resonance cold probe. NMR data processing and analysis were performed using Felix 98.0 (Felix NMR) and Sparky,[20] respectively. Backbone ^{1}H, ^{15}N, and ^{13}C resonance assignments for KIX and TAD$^{150-190}$ were made by analyzing two-dimensional ^{1}H-^{15}N HSQC, three-dimensional (3D) CBCA(CO)NH, HNCACAB, and HNCO spectra; assignments for apo KIX were from ref 21. To gain insights into the architecture of the complex, 3D C(CO)NH-TOCSY, 3D ^{15}N-edited NOESY, and 3D ^{13}C-filtered, ^{13}C-edited NOESY spectra were analyzed. Chemical shift perturbations (CSPs) induced by

DOI: 10.1021/acs.biochem.5b00332
Biochemistry 2015, 54, 5439−5446

various ligands were calculated using the formula $\Delta\delta_{av} = \sqrt{\{0.5[(\delta_{HN,bound} - \delta_{HN,free})^2 + 0.04(\delta_{N,bound} - \delta_{N,free})^2]\}}$. NMR titrations for measuring dissociation constants were performed using a 0.15 mM CBP KIX sample at 25 °C. The CSPs induced as a function of added $TAD^{150-190}$ peptide for each peak were fitted independently using nonlinear regression assuming a single binding site using Grace software employing the fitting function $y = A_1(\{x + 1 + A_0 - \sqrt{[(x + 1 + A_0)^2 - 4x]}\}/2)$, where y is the observed CSP at molar ratio x and A_1 and A_0 are the fitted parameters related to the dissociation constant and the CSP at $x = \infty$, respectively. Naphthol AS-E phosphate was purchased from Sequoia Research Products and used in NMR titrations without further purification. Two equivalents of the compound from a 5 mM stock prepared in DMSO was added to the NMR samples in the concentration range of 0.7−0.75 mM, and CSPs were computed as described above.

Isothermal Titration Calorimetry. ITC experiments were conducted on a MicroCal iTC200 calorimeter. Titrations were performed in triplicate at 20 °C in 20 mM sodium phosphate buffer (pH 7.2) and 150 mM NaCl. Proteins were dialyzed overnight against the buffer used for the titrations. CBP KIX was in the cell, while CRTC1-MAML2 $TAD^{150-190}$ was in the syringe at initial concentrations of 0.1 and 2.3 mM. The titration curves were fitted using a sequential two-site binding model in Origin 7.0.

Co-Immunoprecipitation Assays. The experiments were conducted exactly as previously described following overexpression of full-length HA-tagged CBP with full-length Flag-tagged CRTC1-MAML2 or the CRTC1-MAML2 L180P mutant in HEK293T cells.[22] The plasmids encoding the wild-type proteins were generous gifts of M. Montminy and M. Conkright, respectively. The L180P mutation was introduced using the QuikChange II XL kit (Agilent), and the presence of the mutation was confirmed via DNA sequencing.

RESULTS AND DISCUSSION

CRTC1-MAML2 TAD1 Targets the KIX Domain of CBP/p300. Although previous studies identified a segment within CRTC1-MAML2 TAD1 in CBP/p300 recruitment,[18] the region of CBP/p300 involved in TAD1 binding was not known. Sequence analysis of CRTC1-MAML2 TAD1 suggested some similarity between the segment spanning residues 150−185 and the two helical regions that comprise the minimal KIX-binding domain of CREB pKID (Figure S1A). Two CRTC1-MAML2 TAD constructs, with one construct spanning residues 150−190 and the other spanning residues 172−207, were generated and tested for binding to CBP KIX. Both peptides produced similar changes in the NMR spectrum of KIX (Figure S1B), implying that each peptide harbored the essential determinants for binding to KIX. Because the magnitude of the perturbations was slightly greater for $TAD^{150-190}$ than for $TAD^{172-207}$ and because the former peptide could be readily produced on a large scale, all subsequent analyses were conducted with $TAD^{150-190}$ (unless explicitly indicated otherwise, we shall refer to $TAD^{150-190}$ below as simply TAD).

To gain further insight into the interaction, backbone resonances for the TAD-loaded form of KIX were assigned, which allowed for the quantification of backbone chemical shift perturbations (CSPs) and revealed the identities of the associated resonances (Figure 1A,B). These perturbations were nonuniform and significant (≫0.025 ppm), indicative of a specific association. Titrations of KIX with TAD conducted over a wide range of molar ratios caused "shifting" of resonances to new positions as a function of the amount of added ligand, characteristic of a protein−peptide complex with fast dissociation kinetics (Figure 1C). Nonlinear least-squares fitting of the extent of CSP observed as a function of added ligand for five well-resolved, significantly perturbed resonances, including I611, T614, L620, K621, and A632, yielded an average equilibrium dissociation constant (K_d) for the interaction of 21 ± 13 μM (Figure 1C and Figure S3). The KIX binding affinity for the TAD peptide is comparable to those measured for c-Myb (15 μM),[23] although they are weaker than those of phosphorylated KID (pKID; 0.7 μM) of CREB and MLL1 (2−3 μM).[24,25]

CRTC1-MAML2 TAD1 Binds KIX via a Helical Motif within a Conserved Region. To gain complementary insights into KIX binding by CRTC1-MAML2 TAD, we recorded NMR spectra of the TAD in the absence and presence of KIX. In the absence of KIX, the amide proton resonances of the TAD are narrow, poorly dispersed, and uniform in intensity, characteristic of a natively unfolded peptide (Figure 2A). The addition of 1 equivalent of KIX leads to significant perturbations in the position of a subset of resonances accompanied by a broadening of resonance line widths, characteristic of a specific association with a much larger molecular entity (Figure 2A and Figure S2). The increase in amide proton chemical shift dispersion implies folding of the peptide upon binding to KIX.

To quantify the perturbations and to map the KIX-binding interface, the backbone resonances of the TAD were assigned. Large-scale CSPs in the range of 0.5 ppm or well above this level were observed for several residues with the most significant perturbations mapping to the segment spanning residues 172−189 at the C-terminus of the peptide (Figure 2B), implicating this region in direct interactions with KIX. These results are consistent with our findings that the $TAD^{172-207}$ construct could induce similar perturbations in KIX (Figure S1B). To gain insight into the backbone conformation of the segment in direct contact with KIX, the $^{13}C^{\alpha}$ secondary chemical shifts were quantified (Figure 2B). Many (but not all) residues at the KIX interface exhibited secondary chemical shifts (SCSs) in the range of 2 ppm or well above this level, suggesting the presence of a helical segment extending from P175 to T185.

To test whether the KIX-binding segment identified from our analyses was conserved in MAML2 homologues, a multiple-sequence alignment of MAML2 orthologs from a variety of species and the paralogous MAML1 and MAML3 proteins was constructed. This revealed a conserved region spanning residues 172−190 in CRTC1-MAML2 (Figure 2C). Residues at five positions within this 19-residue segment were invariant, while five other positions were characterized by conservative

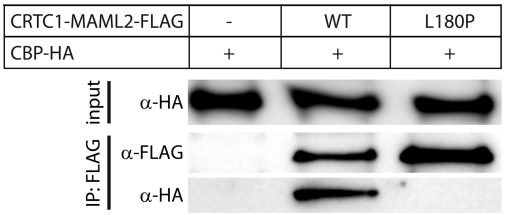

Figure 3. Analysis of the interaction between CRTC1-MAML2 and CBP in cells. Co-immunoprecipitation analyses of HA-tagged CBP protein by Flag-tagged, wild-type, or mutant CRTC1-MAML2. Cell lysates (input) and the immunoprecipitated proteins (IP) were resolved by SDS−PAGE and visualized by Western blot using anti-HA or anti-Flag antibodies.

DOI: 10.1021/acs.biochem.5b00332
Biochemistry 2015, 54, 5439−5446

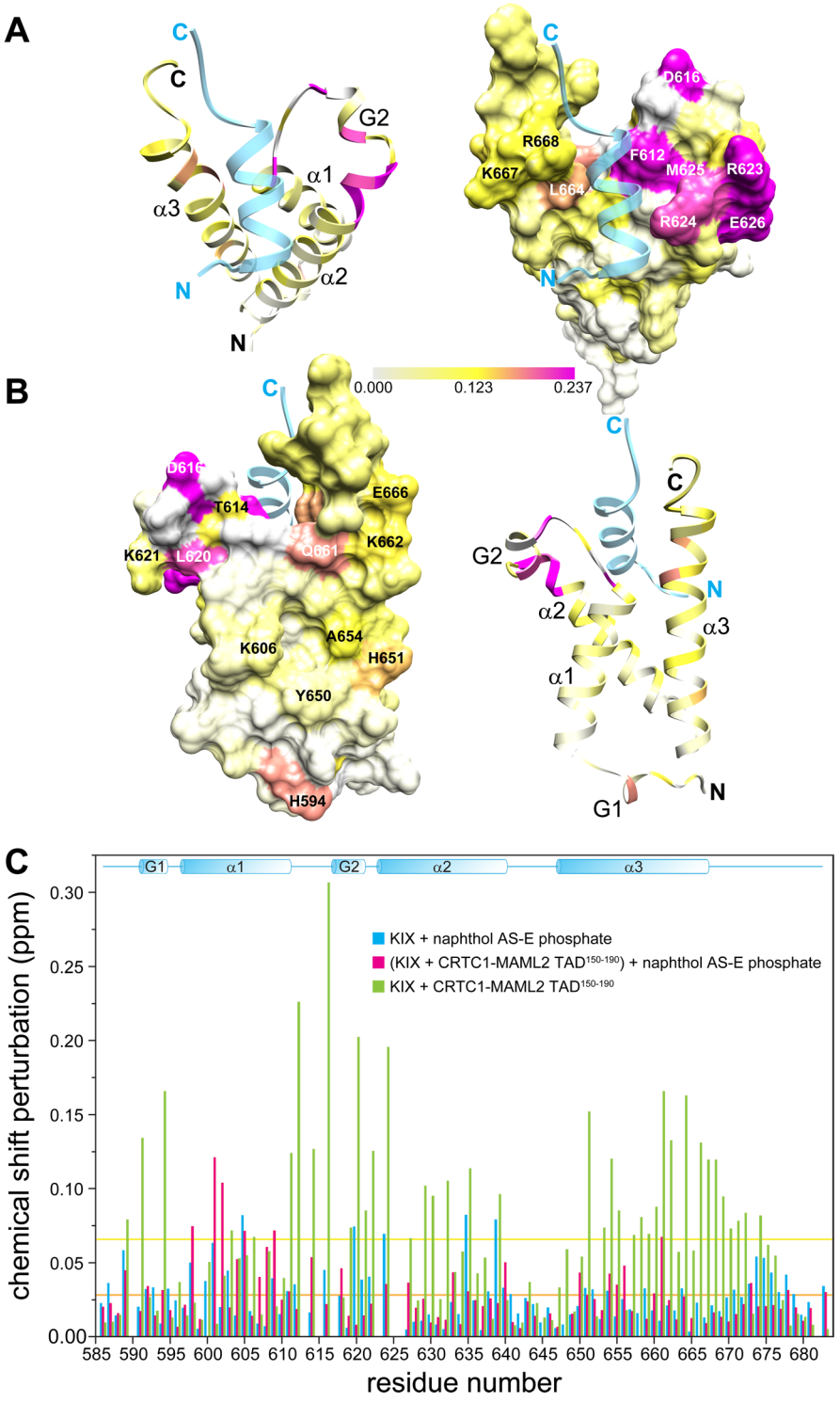

Figure 4. CRTC1-MAML2 TAD1 binds to the MLL1-binding surface of KIX. (A) Backbone amide CSPs induced by CRTC1-MAML2 TAD$^{150-190}$ presented in Figure 1B mapped onto the backbone and molecular surface of KIX (PDB entry 2AGH).[25] The coloring scheme follows the legend shown at the bottom of the panel. Note that KIX residues that show extreme line broadening are rendered with the same color as the maximally perturbed residue. The segment of MLL1 corresponding to residues 844−860 that shows similarity to CRTC1-MAML2 TAD$^{150-190}$ (Figure 2C) is rendered as a semitransparent ribbon. (B) Views of the principal CREB pKID-binding surface of KIX showing the same data as in panel A. (C) CSPs of KIX induced by naphthol AS-E phosphate in the absence (blue) and presence (red) of 1 equiv of CRTC1-MAML2 TAD$^{150-190}$; CSPs induced by CRTC1-MAML2 TAD$^{150-190}$ are included for comparison (green). Protein concentrations as well as solution and experimental conditions were the same as those described in the legend of Figure 1A. The orange and yellow horizontal lines denote the average perturbations induced in KIX by naphthol AS-E phosphate (0.027 ppm for both KIX samples) and by CRTC1-MAML2 TAD$^{150-190}$ (0.066 ppm).

substitutions. This implies that this motif is vital for the function of MAML proteins given that its conservation extends to more than ∼450 million years of evolution.

To evaluate the role of the conserved segment and, in particular, the involvement of a helix in promoting the interaction, we conducted immunoprecipitation experiments with full-length,

DOI: 10.1021/acs.biochem.5b00332
Biochemistry 2015, 54, 5439−5446

Flag-tagged CRTC1-MAML2 and HA-tagged CBP following their expression in HEK293T cells. As expected, CBP failed to be immunoprecipitated when it was expressed alone but was efficiently immunoprecipitated when it is co-expressed with wild-type CRTC1-MAML2 (Figure 3). Because L180 in CRTC1-MAML2 is the centrally located residue within the helical segment that interacts with CBP besides being invariant in MAML2 orthologs (Figure 2C), we mutated this residue to proline with the goal of disrupting the helical structure while concomitantly introducing a nonconservative substitution. Unlike the wild-type protein, the L180P mutant failed to immunoprecipitate CBP (Figure 3), implying that L180 and/or the helical segment played a crucial role(s) in promoting efficient interactions with CBP.

CRTC1-MAML2 TAD1 Binds Primarily to the MLL1-Binding Surface of KIX. To identify the surface targeted by the CRTC1-MAML2 TAD, we mapped the CSPs onto the molecular surface of KIX. Some of the most strongly perturbed residues located in the loop connecting helices α1 and α2, the N-terminus of α2, and the C-terminus of α3 formed a surface that was previously shown to be targeted by MLL1 and FOXO3a (Figure 4A).[25,26] This is confirmed by the observation of intermolecular NOEs between residues in this region of KIX and TAD. Interestingly, the segment of TAD that binds KIX shares some similarity to the MLL1 sequence, at least at those positions in the latter protein known to engage KIX (Figure 2C).[25] Our efforts to determine a high-resolution three-dimensional structure of the CRTC1-MAML2 TAD:CBP KIX complex were thwarted by severe resonance line broadening for several key side chains at the protein-protein interface and the pattern of intermolecular NOEs that suggested more than one binding site for the TAD.

Closer analysis of the CSP maps revealed a secondary binding surface that is distinct from the MLL1 site, comprising residues in the middle and N-terminal portions of the α3 helix and near the N-terminus of the protein (Figure 4B). The latter surface is targeted by CREB pKID and c-Myb, and the pattern of CSPs is reminiscent of that observed for CREB pKID, although the degree of perturbation is much lower in the case of CRTC1-MAML2 TAD.[21] Interestingly, MLL1 and FOXO3a have also been found to bind to this secondary site but with a much lower affinity.[26,27] The fact that this represents a lower-affinity site for CRTC1-MAML2 TAD is suggested by isothermal titration calorimetric analysis (ITC) conducted with KIX and TAD (Figure 1D). The titration data could be readily fitted assuming a two-site binding model with a K_{d1} value of 20 $\pm$ 5 μM and a K_{d2} value of 370 $\pm$ 60 μM. Because the affinity for site 1 is very similar to that measured by NMR (note that all five residues used for NMR measurements are located at or in the vicinity of the MLL1-binding site), we assign the higher-affinity site to the MLL1-binding surface and the lower-affinity site to the pKID-binding surface. This is further supported by the curvilinear trajectories in NMR titrations traced by resonances belonging to residues that straddle the two interfaces including A610 and Q661 [at both the main chain and side chain levels (Figure S3)]. These types of curvilinear trajectories are observed when there are multiple binding sites in the vicinity with widely different binding affinities.[27] Finally, the TAD and pKID share striking similarity at the sequence level, especially in the segment corresponding to the αB helix of pKID (Figure 1A) that engages KIX in this region. We note that the phosphorylated form of a peptide spanning only the αB helix binds KIX with a K_d of 80 μM (an affinity >100-fold lower than that of a phosphopeptide spanning both helices).[23]

To further confirm whether the pKID-binding surface of KIX represents a weaker binding site for the TAD, titrations of naphthol AS-E phosphate, a known allosteric inhibitor of CREB pKID and c-Myb, which binds to an overlapping surface in KIX, were conducted in the absence and presence of the TAD.[28,29] As expected, the compound induced CSPs upon titration with KIX with trends that were similar to those described previously, indicative of a direct association (Figure 4C). The pattern of CSPs suggested that it bound to the surface defined by helices α1 and α2 distinct from both CREB- and MLL1-binding sites, as described previously.[28] However, in the presence of CRTC1-MAML2 TAD, the CSPs induced by the compound were strikingly different with significantly diminished perturbations for residues at or in the vicinity of the MLL1-binding site (residues 620−624), although perturbations for residues in helix α1 comprising its primary binding site were noticeably enhanced (Figure 4C). Importantly, no large-scale CSPs were noted for KIX residues affected by CRTC1-MAML2 TAD binding, especially at or in the vicinity of the MLL1-binding site, implying that the TAD stayed bound to KIX even in the presence of naphthol AS-E phosphate. This was also verified directly by recording spectra for CRTC1-MAML2 TAD in the absence and presence of naphthol AS-E phosphate that resulted in little or no change in the NMR spectrum (Figure S4).

Molecular Model for Collaborative Recruitment of CBP/p300 by CREB and CRTC1/3-MAML2. The results of our studies led us to propose a molecular model for CBP/p300 recruitment by CRTC1/3-MAML2 and CREB (Figure 5).

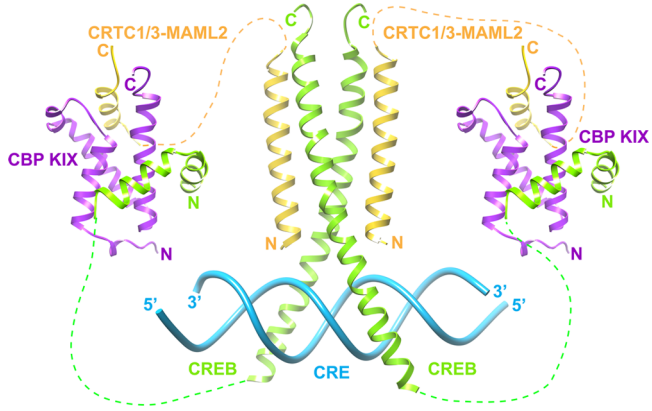

Figure 5. Molecular model for collaborative recruitment of CBP/p300 KIX (purple) at CREs (blue) by CREB (green) and CRTC1-MAML2 (gold). The model is based on the structures of CREB bound to CRE (PDB entry 1DH3),[30] the CREB-binding domain of CRTC2 (PDB entry 4HTM),[10] the MLL1−CBP KIX complex (PDB entry 2AGH),[25] and the CREB−CBP KIX complex (PDB entry 1KDX).[5]

In this model, the N-terminal CBD of CRTC1/3-MAML2 associates with the CRE-bound bZip domain of CREB.[10,30] CRTC1/3-MAML2 TAD1 recruits CBP/p300 KIX by engaging a surface that is distinct from the CREB pKID-binding surface. We note that CREB KID can associate with KIX even when unphosphorylated but with a significantly diminished affinity (~110 μM, which is >100-fold weaker than that of pKID).[23] In the absence of Ser133 phosphorylation, CREB KID could thus collaborate and potentially synergize with CRTC1/3-MAML2 TAD1 to associate with KIX. Indeed, certain KIX interactors, including c-Myb and MLL1, have previously been shown to interact with higher affinity with KIX in this manner.[24] CREB Ser133 phosphorylation by various stimuli, including increases in intracellular cAMP levels, could further enhance the recruitment of CBP/p300 KIX to the promoters of CREB targets. Further studies are needed to explore these possibilities.

DOI: 10.1021/acs.biochem.5b00332
Biochemistry 2015, 54, 5439−5446

■ ASSOCIATED CONTENT

Supporting Information

The Supporting Information is available free of charge on the ACS Publications website at DOI: 10.1021/acs.biochem.5b00332.

Four additional figures (PDF)

■ AUTHOR INFORMATION

Corresponding Author

*Address: 2205 Tech Dr., Evanston, IL 60208-3500. Phone: 847-467-1173. Fax: 847-467-6489. E-mail: i-radhakrishnan@northwestern.edu.

Author Contributions

M.D.C. and G.S.K. are co-first authors because they contributed equally to this work.

Funding

This work was supported by grants from the American Diabetes Association (1-12-BS-168) and the National Institutes of Health (1S10 OD012016) (I.R.). M.D.C. was supported by a Northwestern University Weinberg College of Arts and Sciences Summer Research Grant, and R.M. was supported by a traineeship from the Molecular Biophysics Training Grant (T32 GM008382).

Notes

The authors declare no competing financial interest.

■ ACKNOWLEDGMENTS

We are grateful to Drs. Marc Montminy and Michael Conkright for generously sharing CBP and CRTC1-MAML2 mammalian expression constructs. We are grateful to the Robert H. Lurie Comprehensive Cancer Center at Northwestern University for supporting structural biology research.

■ ABBREVIATIONS

bZip, basic leucine zipper; CREB, cyclic AMP response element-binding protein; CBD, CREB-binding domain; CBP, CREB-binding protein; CRTC, CREB-regulated transcriptional co-activator; CSP, chemical shift perturbation; KID, kinase inducible transactivation domain; pKID, phosphorylated KID; MAML2, Mastermind-like coactivator 2; MBP, maltose-binding protein; MECT, mucoepidermoid carcinoma translocation protein; MLL, mixed lineage leukemia; PCAF, p300/CBP-associated factor; PDB, Protein Data Bank; SCS, secondary chemical shift; TAD, transactivation domain; TEV, tobacco etch virus.

■ REFERENCES

(1) Altarejos, J. Y., and Montminy, M. (2011) CREB and the CRTC co-activators: sensors for hormonal and metabolic signals. *Nat. Rev. Mol. Cell Biol. 12*, 141−151.

(2) Montminy, M. (1997) Transcriptional regulation by cyclic AMP. *Annu. Rev. Biochem. 66*, 807−822.

(3) Chrivia, J. C., Kwok, R. P., Lamb, N., Hagiwara, M., Montminy, M. R., and Goodman, R. H. (1993) Phosphorylated CREB binds specifically to the nuclear protein CBP. *Nature 365*, 855−859.

(4) Parker, D., Jhala, U. S., Radhakrishnan, I., Yaffe, M. B., Reyes, C., Shulman, A. I., Cantley, L. C., Wright, P. E., and Montminy, M. (1998) Analysis of an activator:coactivator complex reveals an essential role for secondary structure in transcriptional activation. *Mol. Cell 2*, 353−359.

(5) Radhakrishnan, I., Perez-Alvarado, G. C., Parker, D., Dyson, H. J., Montminy, M. R., and Wright, P. E. (1997) Solution structure of the KIX domain of CBP bound to the transactivation domain of CREB: a model for activator:coactivator interactions. *Cell 91*, 741−752.

(6) Conkright, M. D., Canettieri, G., Screaton, R., Guzman, E., Miraglia, L., Hogenesch, J. B., and Montminy, M. (2003) TORCs: transducers of regulated CREB activity. *Mol. Cell 12*, 413−423.

(7) Iourgenko, V., Zhang, W., Mickanin, C., Daly, I., Jiang, C., Hexham, J. M., Orth, A. P., Miraglia, L., Meltzer, J., Garza, D., Chirn, G. W., McWhinnie, E., Cohen, D., Skelton, J., Terry, R., Yu, Y., Bodian, D., Buxton, F. P., Zhu, J., Song, C., and Labow, M. A. (2003) Identification of a family of cAMP response element-binding protein coactivators by genome-scale functional analysis in mammalian cells. *Proc. Natl. Acad. Sci. U. S. A. 100*, 12147−12152.

(8) Ravnskjaer, K., Hogan, M. F., Lackey, D., Tora, L., Dent, S. Y., Olefsky, J., and Montminy, M. (2013) Glucagon regulates gluconeogenesis through KAT2B- and WDR5-mediated epigenetic effects. *J. Clin. Invest. 123*, 4318−4328.

(9) Screaton, R. A., Conkright, M. D., Katoh, Y., Best, J. L., Canettieri, G., Jeffries, S., Guzman, E., Niessen, S., Yates, J. R., 3rd, Takemori, H., Okamoto, M., and Montminy, M. (2004) The CREB coactivator TORC2 functions as a calcium- and cAMP-sensitive coincidence detector. *Cell 119*, 61−74.

(10) Luo, Q., Viste, K., Urday-Zaa, J. C., Senthil Kumar, G., Tsai, W. W., Talai, A., Mayo, K. E., Montminy, M., and Radhakrishnan, I. (2012) Mechanism of CREB recognition and coactivation by the CREB-regulated transcriptional coactivator CRTC2. *Proc. Natl. Acad. Sci. U. S. A. 109*, 20865−20870.

(11) Koo, S. H., Flechner, L., Qi, L., Zhang, X., Screaton, R. A., Jeffries, S., Hedrick, S., Xu, W., Boussouar, F., Brindle, P., Takemori, H., and Montminy, M. (2005) The CREB coactivator TORC2 is a key regulator of fasting glucose metabolism. *Nature 437*, 1109−1111.

(12) Kovacs, K. A., Steullet, P., Steinmann, M., Do, K. Q., Magistretti, P. J., Halfon, O., and Cardinaux, J. R. (2007) TORC1 is a calcium- and cAMP-sensitive coincidence detector involved in hippocampal long-term synaptic plasticity. *Proc. Natl. Acad. Sci. U. S. A. 104*, 4700−4705.

(13) Zhou, Y., Wu, H., Li, S., Chen, Q., Cheng, X. W., Zheng, J., Takemori, H., and Xiong, Z. Q. (2006) Requirement of TORC1 for late-phase long-term potentiation in the hippocampus. *PLoS One 1*, e16.

(14) Tonon, G., Modi, S., Wu, L., Kubo, A., Coxon, A. B., Komiya, T., O'Neil, K., Stover, K., El-Naggar, A., Griffin, J. D., Kirsch, I. R., and Kaye, F. J. (2003) t(11;19)(q21;p13) translocation in mucoepidermoid carcinoma creates a novel fusion product that disrupts a Notch signaling pathway. *Nat. Genet. 33*, 208−213.

(15) Fehr, A., Roser, K., Heidorn, K., Hallas, C., Loning, T., and Bullerdiek, J. (2008) A new type of MAML2 fusion in mucoepidermoid carcinoma. *Genes, Chromosomes Cancer 47*, 203−206.

(16) McElhinny, A. S., Li, J. L., and Wu, L. (2008) Mastermind-like transcriptional co-activators: emerging roles in regulating cross talk among multiple signaling pathways. *Oncogene 27*, 5138−5147.

(17) Nam, Y., Sliz, P., Song, L., Aster, J. C., and Blacklow, S. C. (2006) Structural basis for cooperativity in recruitment of MAML coactivators to Notch transcription complexes. *Cell 124*, 973−983.

(18) Wu, L., Liu, J., Gao, P., Nakamura, M., Cao, Y., Shen, H., and Griffin, J. D. (2005) Transforming activity of MECT1-MAML2 fusion oncoprotein is mediated by constitutive CREB activation. *EMBO J. 24*, 2391−2402.

(19) Kumar, G. S., Xie, T., Zhang, Y., and Radhakrishnan, I. (2011) Solution structure of the mSin3A PAH2-Pf1 SID1 complex: a Mad1/Mxd1-like interaction disrupted by MRG15 in the Rpd3S/Sin3S complex. *J. Mol. Biol. 408*, 987−1000.

(20) Goddard, T. D., and Kneller, D. G. (2004) *Sparky 3*, http://www.cgl.ucsf.edu/home/sparky/.

(21) Radhakrishnan, I., Perez-Alvarado, G. C., Parker, D., Dyson, H. J., Montminy, M. R., and Wright, P. E. (1999) Structural analyses of CREB-CBP transcriptional activator-coactivator complexes by NMR spectroscopy: implications for mapping the boundaries of structural domains. *J. Mol. Biol. 287*, 859−865.

(22) Clark, M. D., Marcum, R., Graveline, R., Chan, C. W., Xie, T., Chen, Z., Ding, Y., Zhang, Y., Mondragon, A., David, G., and Radhakrishnan, I. (2015) Structural insights into the assembly of the histone deacetylase-associated Sin3L/Rpd3L corepressor complex. *Proc. Natl. Acad. Sci. U. S. A. 112*, E3669.

DOI: 10.1021/acs.biochem.5b00332
Biochemistry 2015, 54, 5439−5446

(23) Zor, T., Mayr, B. M., Dyson, H. J., Montminy, M. R., and Wright, P. E. (2002) Roles of phosphorylation and helix propensity in the binding of the KIX domain of CREB-binding protein by constitutive (c-Myb) and inducible (CREB) activators. *J. Biol. Chem. 277*, 42241−42248.
(24) Goto, N. K., Zor, T., Martinez-Yamout, M., Dyson, H. J., and Wright, P. E. (2002) Cooperativity in transcription factor binding to the coactivator CREB-binding protein (CBP). The mixed lineage leukemia protein (MLL) activation domain binds to an allosteric site on the KIX domain. *J. Biol. Chem. 277*, 43168−43174.
(25) De Guzman, R. N., Goto, N. K., Dyson, H. J., and Wright, P. E. (2006) Structural basis for cooperative transcription factor binding to the CBP coactivator. *J. Mol. Biol. 355*, 1005−1013.
(26) Wang, F., Marshall, C. B., Yamamoto, K., Li, G. Y., Gasmi-Seabrook, G. M., Okada, H., Mak, T. W., and Ikura, M. (2012) Structures of KIX domain of CBP in complex with two FOXO3a transactivation domains reveal promiscuity and plasticity in coactivator recruitment. *Proc. Natl. Acad. Sci. U. S. A. 109*, 6078−6083.
(27) Arai, M., Dyson, H. J., and Wright, P. E. (2010) Leu628 of the KIX domain of CBP is a key residue for the interaction with the MLL transactivation domain. *FEBS Lett. 584*, 4500−4504.
(28) Best, J. L., Amezcua, C. A., Mayr, B., Flechner, L., Murawsky, C. M., Emerson, B., Zor, T., Gardner, K. H., and Montminy, M. (2004) Identification of small-molecule antagonists that inhibit an activator: coactivator interaction. *Proc. Natl. Acad. Sci. U. S. A. 101*, 17622−17627.
(29) Uttarkar, S., Dukare, S., Bopp, B., Goblirsch, M., Jose, J., and Klempnauer, K. H. (2015) Naphthol AS-E phosphate inhibits the activity of the transcription factor Myb by blocking the interaction with the KIX domain of the coactivator p300. *Mol. Cancer Ther. 14*, 1276.
(30) Schumacher, M. A., Goodman, R. H., and Brennan, R. G. (2000) The structure of a CREB bZIP.somatostatin CRE complex reveals the basis for selective dimerization and divalent cation-enhanced DNA binding. *J. Biol. Chem. 275*, 35242−35247.
(31) Waterhouse, A. M., Procter, J. B., Martin, D. M., Clamp, M., and Barton, G. J. (2009) Jalview Version 2–a multiple sequence alignment editor and analysis workbench. *Bioinformatics 25*, 1189−1191.

DOI: 10.1021/acs.biochem.5b00332
Biochemistry 2015, 54, 5439−5446